ACS APPLIED MATERIALS & INTERFACES

Research Article

www.acsami.org

Surface Functionalization and Electronic Interactions of ZnO Nanorods with a Porphyrin Derivative

Martin Klaumünzer,[‡] Axel Kahnt,*[,¶] Alexandra Burger,[§] Mirza Mačković,[⊥] Corinna Münzel,[‡] Rubitha Srikantharajah,[‡] Erdmann Spiecker,[⊥] Andreas Hirsch,[§] Wolfgang Peukert,[‡] and Dirk M. Guldi*[,¶]

[‡]Institute of Particle Technology, Friedrich-Alexander-University Erlangen-Nuremberg, Cauerstrasse 4, 91058 Erlangen, Germany

[¶]Department of Chemistry and Pharmacy & Interdisciplinary Center for Molecular Materials, Chair of Physical Chemistry I, Friedrich-Alexander-Universität Erlangen-Nürnberg, Egerlandstrasse 3, 91058 Erlangen, Germany

[§]Department of Chemistry and Pharmacy & Interdisciplinary Center for Molecular Materials, Chair of Organic Chemistry II, Friedrich-Alexander-Universität Erlangen-Nürnberg, Henkestrasse 42, 91054 Erlangen, Germany

[⊥]Department of Materials Science and Engineering, Center for Nanoanalysis and Electron Microscopy, Friedrich-Alexander-University, Erlangen-Nuremberg, Cauerstrasse 6, 91058 Erlangen, Germany

Supporting Information

ABSTRACT: To optimize electron transfer and optoelectronic properties in nanoparticulate thin films for electronics we show the surface functionalization of ZnO nanorods by means of replacing surface active 2-[2-(2-methoxyethoxy)-ethoxy]acetic acid (TODA) by a redoxactive organic component, that is, 5,10,15,20-(phenoxyacetat)-porphyrin bearing four carboxylic acids as possible ZnO anchors. Microscopy—transmission electron microscopy—and spectroscopy—optical spectroscopy—verifies the successful and homogenous integration of the porphyrin onto the surface of ZnO nanorods, a process that is facilitated by the four anchoring groups. Photophysical investigations based on emission and absorption spectroscopy prompt to distinct electronic interactions between ZnO nanorods and the porphyrins. Consequently, we performed further photophysical studies flanked by pulse radiolysis assays to corroborate the nature of the electronic interactions.

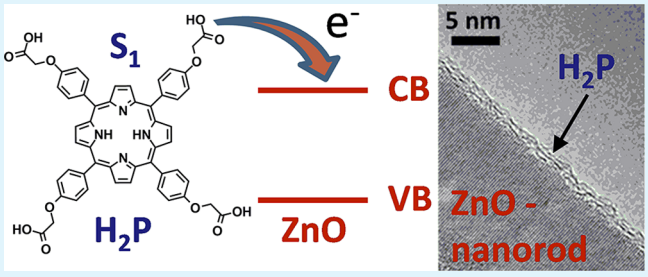

KEYWORDS: *surface functionalization, ZnO nanorods, electronic interactions, redox active porphyrins, laser photolysis, pulse radiolysis*

INTRODUCTION

ZnO is known as a direct band gap (3.37 eV) semiconductor material featuring absorption in the near UV region of the solar spectrum with an exciton binding energy of 60 meV at room temperature.[1,2] Hence, ZnO has emerged as an interesting material for a broad range of optoelectronic thin solid film applications such as solar cells, field effect transistors, etc.[3,4] In these thin solid films, the charge carrier transport across particle-particle interfaces is limited by packing density,[5−7] which sets up a dependence on the particle-particle interfacial potentials. For optimizing electronic interactions at particle-particle interfaces we surface functionalize in this work ZnO nanorods with redox active molecules. This is meant, on one hand, to increase the electron density at the particle-particle interface and, on the other hand, to enhance charge transport processes through thin solid films.

Recently, we demonstrated control over the electronic properties of ZnO nanorods by surface functionalization with a variety of C_{60} phosphonic acid derivatives.[8] We showed that C_{60} acts as an electron acceptor in corresponding ZnO/C_{60} hybrid systems. To gather a better picture on the binding mechanism as well as the adsorption behavior of organics onto nanoparticulates, we present in this work full-fledged microscopic and spectroscopic studies of surface functionalized ZnO nanorods bearing a porphyrin. Owing to the facts that porphyrins are excellent electron donors[9] and that carboxylic acids anchor efficiently to ZnO,[6] we choose 5,10,15,20-(phenoxyacetat)-porphyrin − Figure 1. This allows decisive insights into the optoelectronic characteristics of ZnO/porphyrin systems using steady state and time resolved spectroscopic techniques.

EXPERIMENTAL SECTION

Synthesis. ZnO nanorods were prepared by precipitating zinc acetate dihydrate with potassium hydroxide in methanol and subsequent refluxing for 50 h at 65 °C, as described by Voigt et al.[10] We obtained ZnO nanorods with an average length of ∼100 nm and a diameter of ∼20 nm. Subsequent to their synthesis, ZnO nanorods were surface functionalized with 2-[2-(2-methoxyethoxy)-ethoxy]acetic acid (TODA) to stabilize the dispersions of individual nanorods.[5] The porphyrin was synthesized in a multiple-step procedure, which will be reported elsewhere.[11] TODA, which attached to ZnO nanorods, was exchanged by the porphyrin. To this end, the

Received: January 22, 2014
Accepted: March 25, 2014
Published: March 25, 2014

   dx.doi.org/10.1021/am5004552 | ACS Appl. Mater. Interfaces 2014, 6, 6724−6730

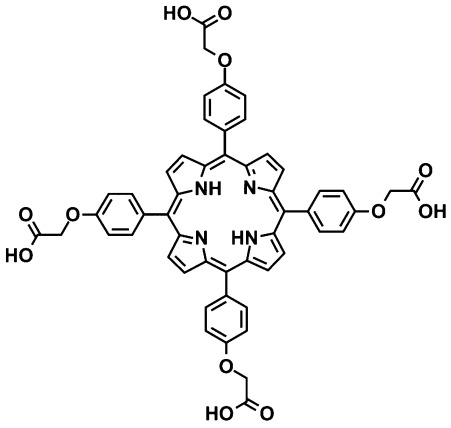

Figure 1. Chemical structure of 5,10,15,20-(phenoxyacetat)-porphyrin (**A**) bearing four carboxylate groups as potential anchors.

porphyrin was dissolved in a trishydroxymethylaminomethane (TRIS) buffer at pH 8, while the TODA functionalized ZnO nanorods were dispersed in TRIS buffer solutions. The suspensions were mixed and ultrasonicated for 60 min. In the first washing step, the suspension was centrifuged and then redispersed with a TRIS buffer to remove the excess of the porphyrin. The second washing step, which involves centrifugation and redispersing in ethanol, was needed to remove the dissolved TODA.

Analytical Methods. Transmission electron microscopy (TEM) was performed using a CM300 UltraTWIN (Philips, Netherlands), equipped with a LaB6 filament and a nominal point resolution of 1.7 Å at the Scherzer defocus. The microscope was operated at an acceleration voltage of 300 kV. TEM images were recorded with a charged coupled device camera (TVIPS, Germany), which has an image size of 2048 × 2048 pixels. TEM samples were prepared by dropping the ZnO dispersions onto Cu grids coated with a holey carbon film layer. During the TEM investigations ZnO nanorods and porphyrins were stable under electron beam irradiation without leading to any appreciable beam damage. The free available software ImageJ (version 1.48r) was used for image analysis. The software JEMS (version 3.5505U2010)[12] and the inorganic crystal structure database (ICSD) were used for identification of the sample material.

Photophysical and Radiation Chemical Methods. UV-vis absorption spectra were recorded on a Varian Cary 5000 spectrophotometer. Photoluminescence (PL) spectra were measured using a FluoroMax P spectrofluorometer (Horiba Jobin Yvon). Photoluminescence lifetimes were determined by the Time Correlated Single Photon Counting technique using a FluoroLog3 emission spectrometer (Horiba Jobin Yvon) equipped with a R3809U-58 MCP (Hamamatsu) and a N-405L laser diode (Horiba Jobin Yvon) exciting at 403 nm (≤200 ps FWHM). Transient absorption measurements based on fs-laser photolysis were carried out with a CPA-2101 femtosecond laser (Clark MXR: output 775 nm, 1 kHz, and 150 fs pulse width) using a transient absorption pump/probe detection system (TAPPS Helios, Ultrafast Systems). The excitation wavelength was either generated by third harmonic generation (258 nm) or using a NOPA (NOPA Puls − Clark MXR) (550 nm). For both excitation wavelengths, pulse widths of <150 fs and energies of 200 nJ/pulse (550 nm) and 40 nJ/pulse (258 nm) were selected. Nanosecond transient absorption laser photolysis measurements were either performed with the output from the third harmonic (355 nm) of an Nd/YAG laser (Brilliant B, Quantel) or with the output from an OPO (Rainbow VIR − Opotek/Quantel, output: 550 nm) pumped by the third harmonic (355 nm) of an Nd/YAG laser (Brilliant, Quantel). For both excitation wavelengths widths of <5 ns and energies of 10 mJ/pulse were selected. The optical detection is based on a pulsed (pulser MSP 05 − Müller Elektronik Optik) Xenon lamp (XBO 450, Osram), a monochromator (Spectra Pro 2300i, Acton Research), a R928 photomultiplier tube (Hamamatsu Photonics), or a fast InGaAs photodiode (Nano 5, Coherent) with 300-MHz amplification, and a 1-GHz digital oscilloscope (WavePro7100, LeCroy). Pulse radiolysis experiments were performed irradiating the samples with electron pulses (1 MeV, 15 ns duration) generated by a pulse transformer electron accelerator ELIT (Institute of Nuclear Physics, Novosibirsk, Russia). The dose delivered per pulse was determined with the help of electron dosimetry and set to 100 Gy. The detection of the transient species was carried out using optical absorption technique, consisting of a pulsed (pulser MSP 05 − Müller Elektronik Optik) xenon lamp (XBO 450, Osram), a SpectraPro 500 monochromator (Acton Research Co), a R9220 photomultiplier (Hamamatsu Photonics), and a 500 MHz digitizing oscilloscope (TDS 640, Tektronix). A more detailed description of the experimental setup was previously published.[13] All pulse radiolysis measurements were conducted in N_2-saturated, aqueous solutions containing 5 vol % *t*-butanol. Such conditions lead to the production of three highly reactive species, namely $^{\bullet}H$, $^{\bullet}OH$, and e_{aq}^-, besides molecular products such as H_2 and H_2O_2. The function of *t*-butanol is to scavenge efficiently $^{\bullet}OH$ and $^{\bullet}H$ radicals via hydrogen abstraction. The main resulting radical $^{\bullet}CH_2(CH_3)_2COH$ is redox inert. Under such conditions the only remaining redox active intermediate is the strongly reducing e_{aq}^-.

RESULTS AND DISCUSSION

Synthesis. Figure 1 sketches the structure of the porphyrin (**A**) featuring four carboxylic acids groups in the periphery to facilitate anchoring to ZnO surfaces.

The synthesis of ZnO nanorods leaves OH- and acetate-terminated surfaces behind,[10] which, in turn, are functionalized by TODA leading to well-stabilized nanorod dispersions as described by Schäfer et al.[5] A subsequently performed ligand exchange enables the successful surface functionalization of the ZnO nanorods with porphyrin **A** − Figure 1. In this context, we expected to displace a maximum of four TODA molecules by a single porphyrin driven at least through the initial phase by entropic effects.

Transmission Electron Microscopy. Figure 2 displays high-resolution-TEM (HRTEM) images of TODA-functionalized ZnO nanorods (Figure 2a) and ZnO nanorods functionalized with **A** (Figure 2b). Figure 2a corroborates that prior to ZnO surface functionalization with **A** no organics were discernable. Considering that TODA stretches approximately 2 nm in length, a totally flat adsorption at the ZnO surface is in accordance with theories published by Knoll.[14] Implicit in the latter is that the oxygen in TODA binds to the acetate/OH terminated surfaces of ZnO via hydrogen bonding yielding a coplanar orientation of TODA with respect to the ZnO surface. On the contrary, if TODA would have been perpendicular with respect to the ZnO surface an organic shell would have been detected.

The interplanar lattice spacing of 0.28 nm corresponds to (10-10) planes of hexagonal ZnO (ICSD 34477). Additionally, XRD-measurements were carried out to confirm the hexagonal wurtzite structure of the ZnO nanorods (not shown). Figure 2b confirms that after surface functionalization of the ZnO nanorods the porphyrins are successfully bound. To this end, an appreciable organic layer, which is present at the ZnO interface, is discernable.

However, a simple physisorption of the porphyrin to the ZnO surface is excluded for the following reasons. Even after multiple washing steps with diverse solvents and with centrifugation−see the Experimental Section for more details−we note significant porphyrin features in the absorption spectra. In Figure 2b, the (0002) lattice planes are visible featuring an interplanar spacing of 0.26 nm. Hence, the long axis of the ZnO rods is parallel to the [0001] direction, as indicated in Figure 2b.

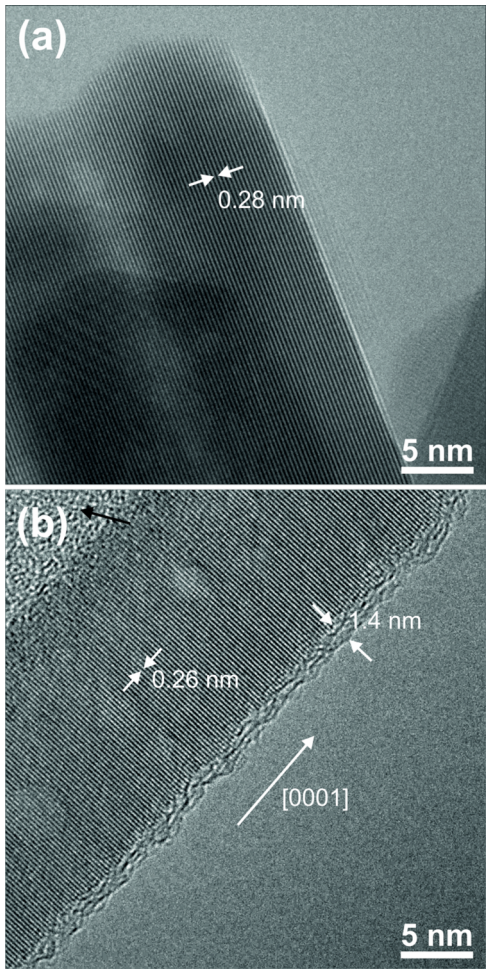

Figure 2. HRTEM images of (a) TODA-functionalized ZnO nanorods and (b) porphyrin-functionalized ZnO nanorods. The interplanar lattice spacing of 0.28 nm in (a) and of 0.26 nm in (b) correspond to (10-10) and (0002) planes of the ZnO wurtzite structure, respectively. The black arrow in (b) points on the amorphous carbon film of the TEM grid and does not relate to the porphyrin.

From the HRTEM measurements (Figure 2b), a homogenous amorphous coating with an average thickness of 1.4 nm was observed, giving some insights into the binding geometry of the porphyrins. In particular, all four carboxylic acid anchors bind to the ZnO surface (see Figure 3).

Please note that such a binding geometry is in accordance with calculations on face to face versus parallel binding.[15] In this context, we assume from the length of the aromatic linker including the carboxylate group as 1.4 nm[16] that the latter stands perpendicularly with respect to the ZnO surface. Thus,

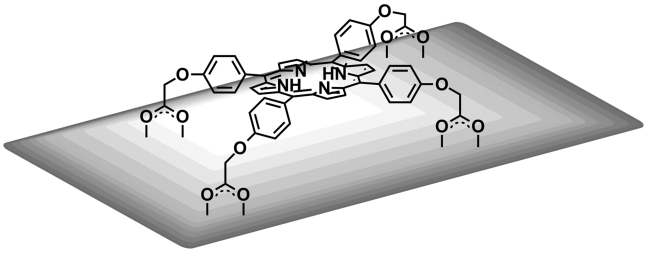

Figure 3. Proposed face-to-face binding geometry of the porphyrin with respect to the ZnO nanorod surface (grey).

the porphyrins arrange—due to the fact that the alpha C is sp^3 hybridized and therefore freely rotatable and flexible—as monolayers in a face-to-face fashion, that is, cofacial with respect to the ZnO nanorod surface.[17,18] Our HRTEM results are overall in good agreement with theoretical considerations in the literature and, as such, document the equal bindings of all four anchors without any intrinsic steric hindrance.[15,16]

Photophysical and Radiation-Chemical Investigations of TODA-Functionalized ZnO Nanorods and Porphyrin-Functionalized ZnO Nanorods. The absorption spectrum of a dispersion containing TODA-functionalized ZnO nanorods is characterized by a dominant absorption in the UV range with an absorption that starts at 373 nm corresponding to the ZnO band edge. In the visible range, light scattering emerges, which originates from partly agglomerated ZnO particles. In addition, TODA-functionalized ZnO nanorods and porphyrin-functionalized ZnO nanorods strongly absorb at 364 nm (3.40 eV) and 365 nm (3.39 eV), respectively – Figure 4. These values agree

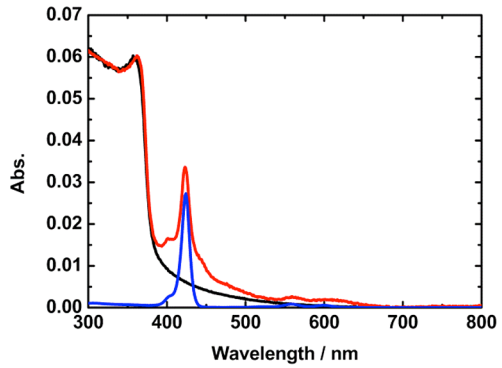

Figure 4. Absorption spectra of TODA-functionalized ZnO nanorods (black), porphyrin-functionalized ZnO nanorods (red), and porphyrin A (blue) in aqueous phosphate buffer solutions of pH 7.2.

reasonably well with literature values regarding the band gap of 3.37 eV for ZnO bulk at room temperature.[2,19] TODA lacks any significant absorption in the range from 260 to 800 nm owing to the fact that its characteristic absorption is around a 220 nm maximum—see SI, Figure S1—deeply in the UV region of the solar spectrum.

Turning to the photoluminescing properties of TODA-functionalized ZnO nanorods photoexcitation with UV light (SI, Figure S2) leads to a photoluminescence spectrum with two distinct bands maximizing at 378 and 545 nm. The peak at the earlier wavelength is attributed to the intrinsic band gap emission via exciton recombination,[20,21] while the latter is attributed to emission resulting from defect states.[21]

When exciting TODA-functionalized ZnO nanorods in H_2O with 258 nm femtosecond laser pulses, an instantaneous formation of a transient absorption in the NIR region with a 820 nm maximum is accompanied by a bleaching in the visible with a 570 nm minimum. Due to the fact that the latter region lacks ground state absorption is interpreted as stimulated photoluminescence (Figure 5 upper part). The common interpretation of the transient absorption in the NIR region is related to conduction band electrons.[22]

In fact, the intraband transitions within the ZnO conduction band are observed,[8] while the stimulated emission comes from exciton recombination.[21] Fitting the decay dynamics, especially that of the stimulated emission and the transient absorption (Figure 5 lower part), by means of a global fit to a biexponential

dx.doi.org/10.1021/am5004552 | ACS Appl. Mater. Interfaces 2014, 6, 6724–6730

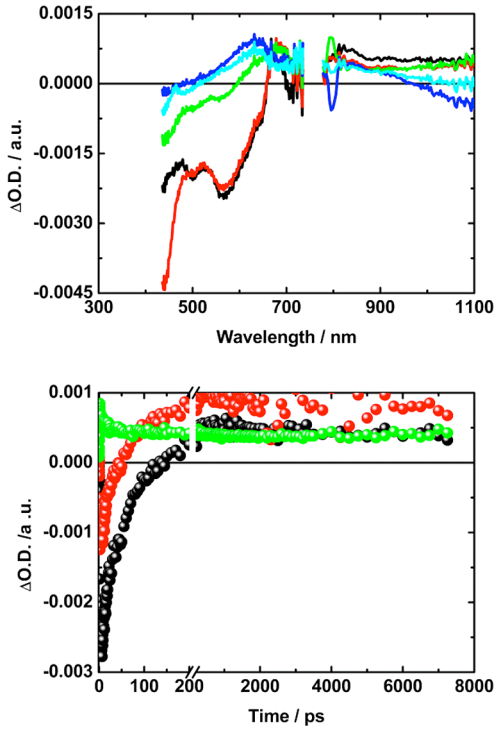

Figure 5. Upper part: Differential absorption spectra (visible and near-infrared) obtained upon femtosecond flash photolysis (258 nm) of TODA-functionalized ZnO nanorods in H_2O with time delays of 1 ps (black), 10 ps (red), 100 ps (green), 1000 ps (blue), and 7250 ps (cyan) at room temperature. Lower part: Corresponding absorption time profiles of the spectra shown above at 570 nm (black), 640 nm (red), and 820 nm (green).

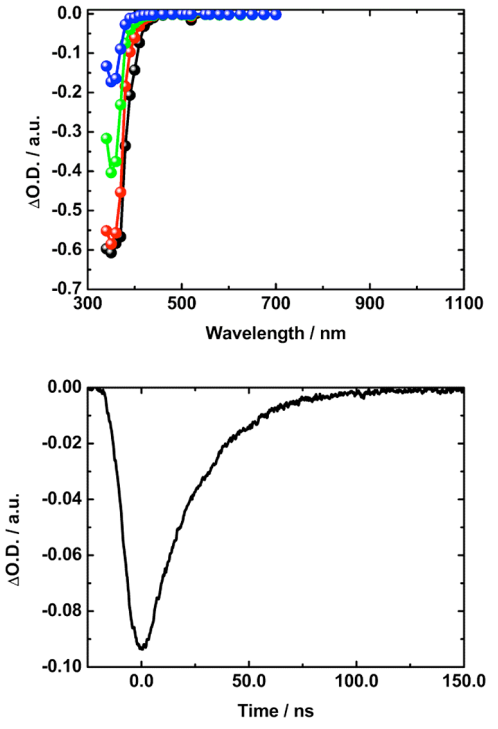

Figure 6. Upper part: Differential absorption spectra obtained upon nanosecond pump probe excitation of TODA-functionalized ZnO nanorods at 355 nm in argon saturated aqueous phosphate buffer solutions of pH 7.2 with time delays of 25 ns (black), 50 ns (red), 75 ns (green), and 100 ns (blue). Lower part: Corresponding absorption time profile at 370 nm.

fitting function results in a short-lived and a long-lived component with time constants of 0.9 and 64 ps, respectively. Whereas the short-lived component is attributed to the thermalization of conduction band electrons, the long-lived component is likely to relate to trapped electrons. The decay of the stimulated emission, which gives rise to a long-lived 640 nm maximum, is best rationalized in terms of a transient absorption of electrons, which reside in trap states.[23,24] Notable, the latter is stable on the time scale of our femtosecond experiments (i.e. up to 8 ns). In light of the aforementioned we turned to nanosecond transient absorption spectroscopy, in which we excited the TODA-functionalized ZnO nanorods at 355 nm. Here, the transient absorption spectrum (Figure 6 upper part) is dominated by a transient bleaching, which minimizes around 360 nm and which mirror images the band gap transition. It results from trapped electrons and holes. These are generated by laser excitation and recover with a lifetime of 25 ns (Figure 6 lower part).

Turning to the reference porphyrin **A** and the porphyrin-functionalized ZnO nanorods: Typically, the absorption spectra of porphyrins reveal a Soret band absorption resulting from $S_0 \rightarrow S_2$ transitions around 420 nm and Q band absorptions originating from $S_0 \rightarrow S_1$ transitions between 500 and 650 nm.[25,26] Minor shifts evolve from the particular substituents.[27] To this end, porphyrin **A** exhibits in aqueous buffer solutions a Soret band absorption at 424 nm accompanied by Q band absorptions at 520, 559, 598, and 652 nm. Surface functionalized ZnO nanorods show, even after multiple washing steps, a marked Soret band absorption at 426 nm. It is safe to postulate that the latter relates to porphyrin **A**. As a matter of fact, the absorption spectrum of porphyrin-functionalized ZnO nanorods is best described as the superposition of the absorptions due to the porphyrin and the ZnO nanorods – Figure 4. This prompts to the hypothesis that, in the ground state, no major interactions occur between ZnO nanorods and the porphyrins. A subtle broadening in the Q-band region evolves, which stems most likely from the fact that the porphyrins lay flat on the ZnO nanorod surface leading to a perturbation of the π system of the porphyrin.

First insights into potential electron donor–acceptor interactions, that is, between ZnO nanorods and the porphyrin came from fluorescence assays. The bare porphyrin, which was used as a reference, exhibits strong fluorescence features between 600 and 800 nm maximizing at 662 and 726 nm – Figure 7. For the porphyrin, a fluorescence quantum yield of 0.055 and a fluorescence lifetime of 7.1 ns were determined in aqueous phosphate buffer solutions of pH 7.2 with H_2TPP (0.11) and ZnTPP (0.03) as references – Figure 8.[28]

Turning to the porphyrin-functionalized ZnO nanorods the shape of the fluorescence spectra upon 550 nm excitation is essentially identical to what has been seen for the porphyrin. Nevertheless, the porphyrin centered fluorescence is quenched with a quantum yield of 7.9×10^{-3}. Likewise, the lifetime of the porphyrin centered fluorescence is with 1.2 ns markedly shorter than in the reference experiment – Figure 8. Strong fluorescence quenching in the porphyrin-functionalized ZnO nanorods prompts to an additional mechanism, that is, electron or energy transfer, by which the porphyrin singlet excited state decays in the presence of the ZnO nanoparticles.

Next, transient absorption spectroscopy based on femtosecond and nanosecond pump probe experiments were

dx.doi.org/10.1021/am5004552 | ACS Appl. Mater. Interfaces 2014, 6, 6724–6730

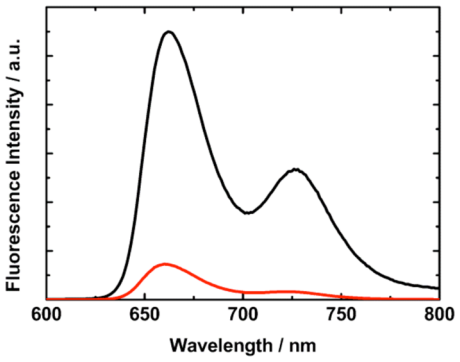

Figure 7. Fluorescence spectra of porphyrin **A** (black) and porphyrin-functionalized ZnO nanorods (red) in aqueous phosphate buffer solutions of pH 7.2 upon photoexcitation at 550 nm.

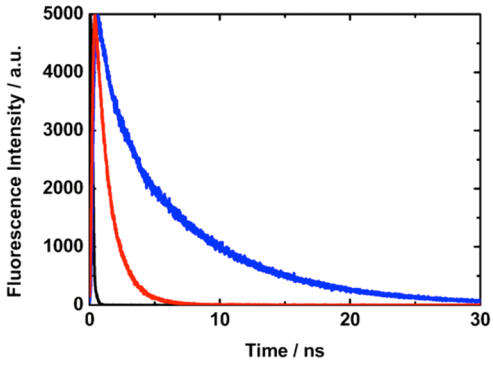

Figure 8. Fluorescence time profiles for porphyrin (blue) and porphyrin-functionalized ZnO nanorods (red), obtained in aqueous phosphate buffer solutions of pH 7.2 recorded at 650 nm, upon 403 nm photoexcitation. The IRF is shown in black.

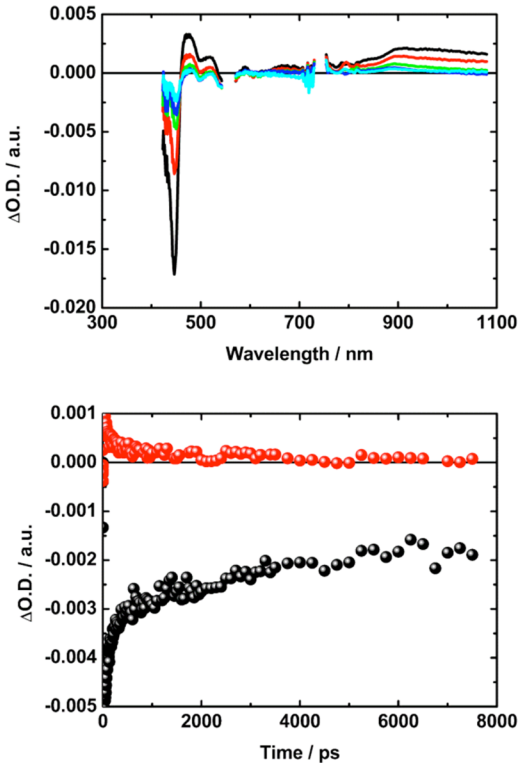

Figure 9. Upper part: Differential absorption spectra obtained upon femtosecond pump probe excitation of porphyrin-functionalized ZnO nanorods at 550 nm in argon saturated aqueous phosphate buffer solutions of pH 7.2 with time delays of 1 ps (black), 10 ps (red), 100 ps (green), 1000 ps (blue), and 7500 ps (cyan). Lower part: Corresponding absorption time profiles at 435 nm (black) and 475 nm (red).

performed to gather evidence for the electron transfer deactivation. For the porphyrin **A** reference, the singlet excited state is formed right after the laser pulse giving rise to maxima at 440, 545, 630, 700, 760, and 1000 nm as well as minima at 525, 565, and 660 nm. Please note that the latter mirror the ground state absorption – Figure S3. Overall, the transient features decay with a lifetime of 7.0 ns to afford the corresponding triplet manifold, for which maxima at 460, 540, 620, and 675 nm as well as minima at 520, 560, and 645 nm evolve – Figure S3.

The corresponding differential absorption spectra recorded upon photoexcitation of porphyrin-functionalized ZnO nanorods includes broad transient absorption signatures in the visible and the near-infrared of the solar spectrum. In particular, maxima at 475, 515, 590, 625, and 915 nm and minima at 440, 500, 525, 610, 640, and 915 nm are excellent matches to what has been recorded for just the singlet excited state of the porphyrin.[29] Unlike the porphyrin, whose singlet excited state decays with a lifetime of 7.0 ns in the absence of any ZnO nanoparticulates—vide supra—now a lifetime of 1.1 ns was derived. Within this lifetime, a differential absorption spectrum evolves featuring maxima at 480, 520, 590, and 890 nm complemented by minima at 430, 450, and 500 nm. In total, these match the characteristic fingerprints of one electron oxidized porphyrin, $H_2TPP^{\bullet+}$ – Figure 9.[25,30]

Taking the aforementioned into concert, we postulate an electron transfer from the singlet excited state of the porphyrin into the conduction band of ZnO nanorods forming a porphyrin$^{\bullet+}$-ZnO$(e_{CB})^-$ charge separated state. Notable is in this context that past investigations have unambiguously documented the favorable driving force for the charge injection.[15,31] The transient absorption spectra upon nanosecond photolysis exciting exclusively the porphyrin at 550 nm are dominated by transient bleaching at 360, 420, and 550 nm (Figure 10 upper part) mirroring the ground state absorption of the porphyrin-functionalized ZnO nanorod. A multiwavelength analysis documents that this charge separated state recombines with a lifetime of 31 ns and reinstates the ground state – Figure 10. Noteworthy is at this point the lack of transient absorptions that might corroborate the newly injected electrons in the ZnO conduction band.

To verify the injection of electrons from the porphyrin singlet excited state into the conduction band of ZnO pulse radiolysis experiments were performed with TODA-functionalized ZnO nanorods under reducing conditions. The bimolecular reaction between TODA-functionalized ZnO nanorods and e_{aq}^- was followed by monitoring the 720 nm absorption maximum of the latter. Its decay gives rise to a new transient species in the ultraviolet region, that is, a 360 nm minimum. A closer analysis of the 360 nm minimum discloses its match with the band gap transition of ZnO nanoparticulates – Figures 11 and S4. As such, we ascribe the transient absorption changes to correlate with the product of electron injection into the conduction band of ZnO nanorods.

As the concentration of the ZnO single rod reference was increased, which was reflected by the increased absorption at 360 nm from 0.29 to 1.10, the respective first-order rate constant for the decay of e_{aq}^- reveals a linear relationship with

dx.doi.org/10.1021/am5004552 | ACS Appl. Mater. Interfaces 2014, 6, 6724–6730

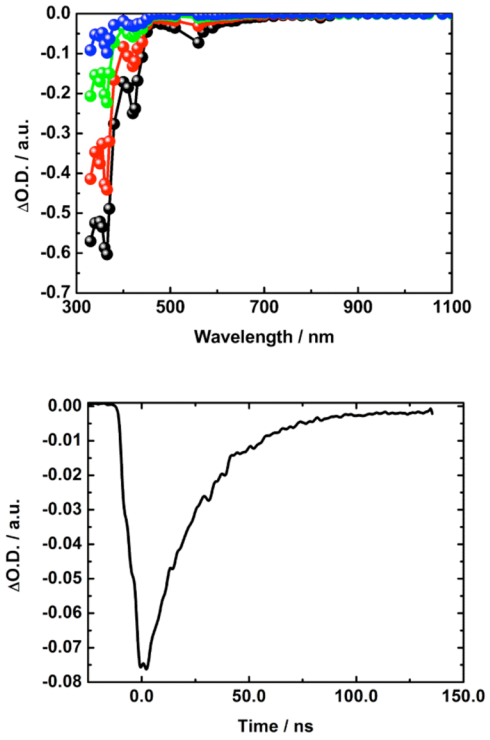

Figure 10. Upper part: Differential absorption spectra obtained upon nanosecond pump probe excitation of porphyrin-functionalized ZnO nanorods at 550 nm in argon saturated aqueous phosphate buffer solutions of pH 7.2 with time delays of 25 ns (black), 50 ns (red), 75 ns (green), and 100 ns (blue). Lower part: Corresponding absorption time profile at 420 nm.

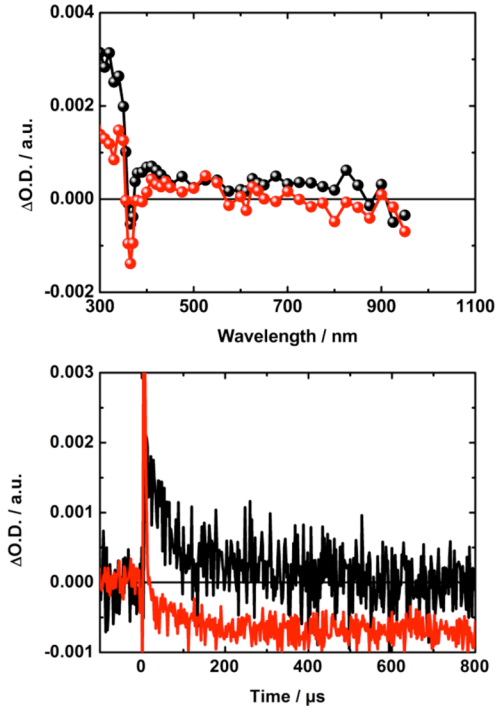

Figure 11. Upper part: Differential absorption spectra obtained upon electron pulse radiolysis (100 Gy, 15 ns FWHM) of TODA-functionalized ZnO nanorods in nitrogen saturated aqueous solution containing 5 vol % t-butanol with time delays of 50 μs (black) and 150 μs (red). Lower part: Corresponding absorption time profiles at 300 nm (black) and 360 nm (red).

respect to the ZnO single rod concentration. Plotting the pseudo-first-order rate constant k_{obs} vs the optical absorption of the sample at 360 nm and fitting the data to a linear function a slope of 4.2×10^6 A_{360}^{-1} s^{-1} was obtained (SI, Figure S4).[32] Following the initial ZnO nanorod reduction the transient features in the ultraviolet region decay, while the ground state bleaching at 360 nm further intensifies – Figure 11. We ascribe this process to the shift of electrons that either reside in the conduction band or in near band gap traps to deeper level traps.[33,34] The rate constant for the electron shift into deeper traps was derived from monoexponential fitting of the decays at 300 and 360 nm affording a value of 9×10^3 s^{-1}.

Considering that the newly injected conduction band electron leads to characteristic fingerprints in the ultraviolet region of the solar spectrum is well in line with the femtosecond and nanosecond transient absorption laser photolysis experiments for porphyrin-functionalized ZnO nanorods (Figures 9 and 10) showing no significant ZnO based transient absorption in the visible and NIR region of the solar spectrum.[35]

CONCLUSIONS

We have successfully surface functionalized ZnO nanorods with a photo- and redoxactive organic building block, that is, a porphyrin bearing four carboxylic acids. The latter act as potential anchors to link the porphyrin to the surface of ZnO nanorods in the form of a homogenous, uniform, and amorphous monolayer. Detailed photophysical and radiation chemical assays corroborate an efficient electron injection from the porphyrin singlet excited state into the conduction band of the ZnO nanorods. The correspondingly formed charge separated state decays by either charge recombination or trapping electrons into different trap states. We believe that our findings offers a myriad of incentives towards research in the emerging areas of ZnO based nanomaterials such as optoelectronics, solar light conversion, or printable electronics.

ASSOCIATED CONTENT

Supporting Information

UV-vis spectra, photoluminescence spectra, fs-laser photolysis transient absorption spectra, pulse radiolysis transient absorption spectra, time profiles, and Stern–Volmer plot. This material is available free of charge via the Internet at http://pubs.acs.org.

AUTHOR INFORMATION

Corresponding Authors

*E-mail: dirk.guldi@fau.de.
*E-mail: axel.kahnt@fau.de.

Author Contributions

The manuscript was written through contributions of all authors. All authors have given approval to the final version of the manuscript. M.K. and A.K. contributed equally to this paper.

Notes

The authors declare no competing financial interest.

ACKNOWLEDGMENTS

The authors thank the Deutsche Forschungsgemeinschaft DFG for financial support via the Cluster of Excellence "Engineering of Advanced Materials (EAM)" and the Research Training Group "Disperse Systems for Electronics" 1161/2. A.K.

acknowledges gratefully funding from the DFG via grant KA 3491/2-1. We would like to thank Prof. Abel and his group from the Leipzig University, Leipzig, Germany, for the support during the pulse radiolysis measurements.

■ ABBREVIATIONS

TODA = 2-[2-(2-methoxyethoxy)ethoxy]acetic acid, porphyrin **A** 5,10,15,20-(phenoxyacetat)-porphyrin
TRIS = trishydroxymethylaminomethane

■ REFERENCES

(1) Özgür, Ü.; Alivov, Y. I.; Liu, C.; Teke, A.; Reshchikov, M. A.; Doğan, S.; Avrutin, V.; Cho, S.-J.; Morkoc, H. A Comprehensive Review of ZnO Materials and Devices. *J. Appl. Phys.* **2005**, *98*, 041301−103.
(2) Janotti, A.; van de Walle, C. G. Fundamentals of Zinc Oxide as a Semiconductor. *Rep. Prog. Phys.* **2009**, *72*, 126501−29.
(3) Marczak, R.; Werner, F.; Ahmad, R.; Lobaz, V.; Guldi, D. M.; Peukert, W. Detailed Investigations of ZnO Photoelectrodes Preparation for Dye Sensitized Solar Cells. *Langmuir* **2011**, *27*, 3920−3929.
(4) Faber, H.; Klaumünzer, M.; Voigt, M.; Galli, D.; Vieweg, B. F.; Peukert, W.; Spiecker, E.; Halik, M. Morphological Impact of Zinc Oxide Layers on the Device Performance in Thin-film Transistors. *Nanoscale* **2011**, *3*, 897−899.
(5) Schäfer, S.; Srikantharajah, R.; Klaumünzer, M.; Lobaz, V.; Voigt, M.; Peukert, W. Self-Alignment of Zinc Oxide Nanorods into a 3D-Smectic Phase. *Thin Solid Films* **2014**, submitted.
(6) Liu, D.; Wu, W.; Qiu, Y.; Yang, S.; Xiao, S.; Wang, Q.; Ding, L.; Wang, J. Surface Functionalization of ZnO Nanotetrapods with Photoactive and Electroactive Organic Monolayers. *Langmuir* **2008**, *24*, 5052−5059.
(7) Thiemann, S.; Gruber, M.; Lokteva, I.; Hirschmann, J.; Halik, M.; Zaumseil, J. High-Mobility ZnO Nanorod Field-Effect Transistors by Self-Alignment and Electrolyte-Gating. *J. Appl. Mater. Interfaces* **2013**, *5*, 1656−1662.
(8) Voigt, M.; Klaumünzer, M.; Ebel, A.; Werner, F.; Yang, G.; Marczak, R.; Spiecker, E.; Guldi, D. M.; Hirsch, A.; Peukert, W. Surface Functionalization of ZnO Nanorods with C60 Derivatives Carrying Phosphonic Acid Functionalities. *J. Phys. Chem. C* **2011**, *115*, 5561−5565.
(9) Aloukos, P.; Iliopoulos, K.; Couris, S.; Guldi, D. M.; Sooambar, C.; Mateo-Alonso, A.; Nagaswaran, P. G.; Bonifazi, D.; Prato, M. Photophysics and Transient Nonlinear Optical Response of Donor−[60]Fullerene Hybrids. *J. Mater. Chem.* **2011**, *21*, 2524−2534.
(10) Voigt, M.; Klaumünzer, M.; Thiem, H.; Peukert, W. Detailed Analysis of the Growth Kinetics of ZnO Nanorods in Methanol. *J. Phys. Chem. C* **2010**, *114*, 6243−6249.
(11) Burger, A.; Costa, R.; Lobaz, V.; Peukert, W.; Guldi, D. M.; Hirsch, A. in preparation.
(12) Stadelmann, P. A.; Jems Electron Microscopy Software, Java Version 3.7624U2012, CIME-EPFL, Switzerland, (1999−2012).
(13) Brede, O.; Orthner, H.; Zubarev, V.; Hermann, R. Radical Cations of Sterically Hindered Phenols as Intermediates in Radiation-Induced Electron Transfer Processes. *J. Phys. Chem.* **1996**, *100*, 7097−7105.
(14) Knoll, S. C. M. Elektrophoretische Formgebung von Nanoskaligem Zirkoniumdioxid. Dissertation, Saarbrücken 2001.
(15) Werner, F.; Gnichwitz, J.-F.; Marczak, R.; Palomares, E.; Peukert, W.; Hirsch, A.; Guldi, D. M. Grafting Porphyrins (Face-to-Edge/Orthogonal versus Face-to-Face/Parallel) to ZnO en Route toward Dye-Sensitized Solar Cells. *J. Phys. Chem. B* **2010**, *114*, 14671−14678.
(16) Martinez-Guajardo, G.; Donald, K. J.; Wittmaack, K. B.; Vazquez, M. A.; Merino, G. Shorter Still: Compressing C−C Single Bonds. *Org. Lett.* **2010**, *12*, 4058−4061.
(17) Ditze, S.; Stark, M.; Buchner, F.; Aichert, A.; Jux, N.; Luckas, N.; Görling, A.; Hieringer, W.; Hornegger, J.; Steinrück, H.-P.; Marbach, H. On the Energetics of Conformational Switching of Molecules at and Close to Room Temperature. *J. Am. Chem. Soc.* **2014**, *136*, 1609−1616.
(18) Guldi, D. M.; Luo, C.; Prato, M.; Troisi, A.; Zerbetto, F.; Scheloske, M.; Dietel, E.; Bauer, W.; Hirsch, A. Parallel (Face-to-Face) Versus Perpendicular (Edge-to-Face) Alignment of Electron Donors and Acceptors in Fullerene Porphyrin Dyads: The Importance of Orientation in Electron Transfer. *J. Am. Chem. Soc.* **2001**, *123*, 9166−9167.
(19) Mang, A.; Reimann, K.; Rübenacke, S. Band Gaps, Crystal-Field Splitting, Spin-Orbit Coupling, and Exciton Binding Energies in ZnO under Hydrostatic Pressure. *Solid State Commun.* **1995**, *94*, 251−254.
(20) Weiher, R. L.; Tait, W. C. Observation of Mixed-Mode Excitons in the Photoluminescence of Zinc Oxide. *Phys. Rev. I* **1969**, *185*, 1114−1116.
(21) Djurisic, A. B.; Leung, Y. H. Optical Properties of ZnO Nanostructures. *Small* **2006**, *2*, 944−961.
(22) Such new conduction band electrons come as part of excitons, that is, strongly bound electron hole pairs and, in turn, are incomparable to the electrons injected in pulse radiolytic reduction experiments and/or from excited state electron donor.
(23) Quist, P. A. C.; Beek, W. E. J; Wienk, M. M.; Janssen, R. A. J.; Savenije, T. J.; Siebbeles, L. D. A. Photogeneration and Decay of Charge Carriers in Hybrid Bulk Heterojunctions of ZnO Nanoparticles and Conjugated Polymers. *J. Phys. Chem. B* **2006**, *110*, 10315−10321.
(24) Ramakrishna, G.; Ghosh, H. N. Effect of Particle Size on the Reactivity of Quantum Size ZnO Nanoparticles and Charge-Transfer Dynamics with Adsorbed Catechols. *Langmuir* **2003**, *19*, 3006−3012.
(25) El-Khouly, M. E.; Ito, O.; Smith, P. M.; D'Souza, F. Intermolecular and Supramolecular Photoinduced Electron Transfer Processes of Fullerene−Porphyrin/Phthalocyanine Systems. *J. Photochem. Photobiol., C* **2004**, *5*, 79−104 and references herein.
(26) Sessler, J. L.; Seidel, D. Synthetic Expanded Porphyrin Chemistry. *Angew. Chem., Int. Ed.* **2003**, *42*, 5134−5175 and references herein.
(27) Weinkauf, J. R.; Cooper, S. W.; Schweiger, A.; Wamser, C. Substituent and Solvent Effects on the Hyperporphyrin Spectra of Diprotonated Tetraphenylporphyrins. *J. Phys. Chem. A* **2003**, *107*, 3486−3496.
(28) Seybold, P. G.; Gouterman, M. Porphyrins: XIII: Fluorescence Spectra and Quantum Yields. *J. Mol. Spectrosc.* **1969**, *31*, 1−13.
(29) Minor deviation is well explained with the fact that **A** is attached to the ZnO surface.
(30) Gasyna, Z.; Browett, W. R.; Stillman, M. J. Pi.-Cation-Radical Formation Following Visible Light Photolysis of Porphyrins in Frozen Solution using Alkyl Chlorides or Quinones as Electron Acceptors. *Inorg. Chem.* **1985**, *24*, 2440−2447.
(31) Niskanen, M.; Kuisma, M.; Cramariuc, O.; Golovanov, V.; Hukka, T. I.; Tkachenko, N.; Rantala, T. T. Porphyrin Adsorbed on the (1010) Surface of the Wurtzite Structure of ZnO − Conformation Induced Effects on the Electron Transfer Characteristics. *Phys. Chem. Chem. Phys.* **2013**, *15*, 17408−17418.
(32) The lack of reliable extinction coefficients or molar concentrations hampers the calculation of a bimolecular rate constant.
(33) Jacobsson, T. J.; Edvinsson, T. A Spectroelectrochemical Method for Locating Fluorescence Trap States in Nanoparticles and Quantum Dots. *J. Phys. Chem. C* **2013**, *117*, 5497−5504.
(34) Schmidt, M.; Ellguth, M.; Karsthof, R.; von Wenckstern, H.; Pickenhain, R.; Grundmann, M.; Brauer, G.; Ling, F. C. C. On the T2 Trap in Zinc Oxide Thin Films. *Phys. Status Solidi B* **2012**, *249*, 588−595.
(35) Notably, the detection system of our fs-laser photolysis setup enables only recording throughout the visible and near-infrared regions of the solar spectrum. Here, porphyrin centered transitions dominate and mask those related to ZnO nanorods including those that relate to newly injected conduction band electrons. In fact, the latter are more likely to be seen in the ultraviolet region of the solar spectrum.